Global Science and Technology Journal
Vol. 6. No. 3. September 2018 Issue. Pp.12-24

Synthesis, Structural and Magnetic Properties of Chromium Substituted Mn-Zn Ferrite

F. Alam*[1], Bablu Chandra Das[2] and A. K. M. Akther Hossain[3]

Substitution of chromium in Mn-Zn ferrite and its effect on structural and magnetic properties has been studied. Samples were synthesized by combustion method and sintered at various temperatures (T_s). XRD patterns indicate that the samples are of single phase cubic spinel structure. The lattice parameter decreases with increase with substitution of Cr^{3+} content. Average grain size (D), bulk density (ρ_B), initial permeability (μ_i'), Néel temperature (T_N) decrease with the increase in chromium content. ρ_B was found to increase with increase in Cr^{3+} content as the T_s is increased. The T_s affect the densification, grain growth and μ_i' of the samples. μ_i' strongly depends on D, density and intragranular porosity. T_N was found to decrease with the increase in Cr^{3+} concentration. This is attributed to the weakening of A-B interaction. The sharp fall of μ_i' at T_N indicates that the compositions are homogeneous. Saturation magnetization (M_s), Coercive field (H_c), Residual induction (B_r) were studied as a function of Cr^{3+} content. The M_s was found to decrease with the increase of Cr^{3+} content, which is attributed to the dilution of A-B interaction. The inclusion of Cr^{3+} caused the M_s, B_r and hysteresis losses to decrease.

Keywords: Combustion method, Saturation Magnetization, Initial Permeability, Intragranular porosity, Coercive field.

1. Introduction

Ferrites are magnetic oxide materials with semiconducting nature which are of great technological importance by virtue of their electrical and magnetic properties. Spinel ferrites are widely used because they possess high electrical resistivity, low eddy current and dielectric losses, high saturation magnetization, high permeability and moderate permittivity. They are used in transformer cores, antenna rods, memory chips, high density magnetic recording media, transducers, activators, permanent magnets, bubble devices, microwave and computer technology (Snelling, 1988; Van Vleck, 1989; Spaldin, 2003).

Most modern soft ferrites have spinel type crystal structure. Ferrites are ferromagnetic substances of double oxides of iron and another metal. It has tetrahedral *A* site and octahedral *B* site in AB_2O_4 crystal structure. Depending on *A* site and *B* site cations it can exhibit ferromagnetic, antiferromagnetic, spin (cluster) glass, and paramagnetic behaviour (Verway and Heilmann, 1947; Goldman, 1990;

[1*]F. Alam, Corresponding Author, Department of Physical Sciences, School of Engineering and Computer Science, Independent University, Bangladesh (IUB), Dhaka, Bangladesh, Email: farhadiub@gmail.com
[2]Bablu Chandra das, Department of Physics, Bangladesh University of Engineering and Technology (BUET), Dhaka, Bangladesh, Email: bcdasbuet@gmail.com
[3]A. K. M. Akther Hossain, Department of Physics, Bangladesh University of Engineering and Technology (BUET), Dhaka, Bangladesh, Email: akmahossain@phy.buet.ac.bd

Craik, 1975). Various cations can be placed in *A* site and *B* site to tune its magnetic properties. In the spinel structure, the magnetic ions are distributed among two different lattice sites, tetrahedral (A) and octahedral (B) sites. The structural, magnetic and electrical properties of these ferrites depend on the relative distribution of cations at the different sites as well as the preparation condition. Combustion technique meets the increasing demand for the synthesis of fine ferrite powders with high density at low temperatures. As a new approach, combustion synthesis is less energy consuming and less polluting than the other techniques of ferrite powder manufacture. Mn–Zn ferrite, one of the main categories of soft magnetic materials has high permeability, low magnetic loss, and high electrical conductivity. Therefore Mn–Zn ferrites are mainly used as the cores for inductors, transformers, recording heads and in switch mode power supplies (Cahn et al., 1994). The properties of Mn–Zn ferrite depend mainly on the technique and conditions of preparation, which in turn affect the cation distribution over the tetrahedral A–site and the octahedral B–sites. Since the research on Mn-Zn ferrites is so vast, it is difficult to collect all experimental results and information about all types of ferrites in every aspect. The systematic research is still necessary for more comprehensive understanding of such materials. In this research a series of ferrites have been prepared to investigate the effect of substitution of trivalent transition metal ion chromium (Cr^{3+}) on the structural and magnetic properties of Mn-Zn ferrite. This paper comprises of five sections. Section 1 is the introduction; section 2 deals with literature review closely related to this article, Section 3 describes the experimental techniques, Section 4 explains the results and possible logical explanation against them and finally the concluding remarks in section 5.

2. Literature Review

Different aspects of base Mn-Zn ferrite and dopant Mn- Zn ferrites on structural, magnetic, electrical, dielectric and applications have been reported by Shokrollahi and Janghorban (2007) and El-Sayed (2006). Substitution of Ni^{2+} ions in Mn-Zn ferrite and its effect on structural, electrical and magnetic properties has been studied by Nam *et al.* (1997) and Yue *et al. (2003)*. Dionne and West (1987) and Singh *et al.* (2004) also have investigated the magnetic and electric properties of Ni^{2+} substituted Mn-Zn ferrites. The structural and magnetic properties of Mn substituted Ni-Mn-Zn ferrites sintered at various temperatures have been studied by Hossain *et al*. (2009). It was observed that the lattice parameters and average grain sizes increase with Mn substitution. The increase in lattice parameter with increasing Mn^{2+} substitution was explained in terms of ionic radii. It was also observed that the real part of initial permeability ($\mu_i^{/}$) increases with increasing Mn content in the Ni-Zn-Mn ferrites. The Cobalt substituted Mn-Zn ferrites have been studied by Babbar and Puri (1992). Ferrite series of the composition Mn-Zn-Co ferrites were prepared by the hot-pressing technique. They got ferrites with improved magnetic properties having low porosity and small grain sizes. From these observations, it is indicated that with increasing sintering temperature, grain growth enhances and the average grain size increases and that grain growth leads to higher permeability, small coercive field, small remanence, small hysteresis loop, rapid response to high-frequency magnetic fields in Mn-Zn ferrite. Pannaparayil et al. (1991) investigated the magnetic properties of high density Mn-Zn ferrites. High densities have been obtained upon sintering these ferrite powders at relatively low temperatures. It is seen that μ_i increases with increase in density. This is attributed to the variation in grain sizes of

the ferrites with temperatures. Mn-Zn ferrites are extensively used in broad band and pulse transformer and wideband read heads for high definition video recording. For use in such devices, initial permeability should remain constant over certain frequency ranges. Here in this case it remains level at first, and then rises to a very shallow maximum before falling rapidly to a relatively low value due to ferromagnetic resonance. It was found that the larger the dc value of the permeability, the lower the frequency at which μ_i begins to drop. Therefore it is fascinating to discuss the effect of Chromium ion on the structural and magnetic properties of Mn-Zn ferrite sintered at different sintering temperatures to achieve the optimum parameters like high saturation magnetization, high permeability, high resistivity, low eddy current loss, etc. along with loss and quality factors of the sample.

3. Methodology

The ferrite powder of $Mn_{0.50}Zn_{0.50}Cr_xFe_{2-x}O_4$ (with x = 0.0-0.4) has been synthesized by auto combustion method. Stoichiometric amounts of commercially available analytical grade powders of $MnCl_2.4H_2O$, $Cr(NO_3)_3.9H_2O$,$Zn(NO_3)_2.6H_2O$and Fe $(NO_3)_3.9H_2O$ were dissolved in ethanol to obtain a mixed homogenous solution. Ammonia solution was slowly added to metal nitrate solution to adjust the pH at 7. The solution was placed at constant temperature bath (~70ºC) followed by an ignition and formed a fluffy loose powders of the desired composition. The resultant powders of the samples were calcined at 700ºC for five hours in air. The grounded fine powders were then pressed into disk- and toroid-shaped samples. The samples prepared from each composition were sintered at 1250, 1300 and 1350ºC for 5 hrs in air. During sintering, temperature ramps were 10ºC /min for heating and 5ºC /min for cooling. The structural characterization was carried out with an X-ray diffractometer using CuK_α radiation (λ = 1.54178Å). The lattice parameter for each composition was determined using Nelson-Riley function (Nelson & Riley, 1945). Bulk densities of the samples were determined using the expression $\rho_B = (W \times \rho)/W - W'$ where W and W' are the weight of the sample in air and water, respectively and ρ is the density of water at room temperature. The theoretical density, ρ_{th}, was calculated using the relation: $\rho_{th} = (ZM/N_A a^3)$, where N_A is Avogadro's number, M is the molecular weight of the corresponding composition, a^3 is the volume of the cubic unit cell and Z is the number of molecules per unit cell, which is 8 for the spinel cubic structure. The percentage porosity, P% was calculated from the relation $P(\%) = \{(\rho_{th} - \rho_B)/\rho_{th}\} \times 100$. For surface morphology, polished and etched samples of different compositions sintered at different temperatures were chosen. The samples were visualized under a high-resolution optical microscope (Olympus DP70). Average grain sizes of the samples were determined from optical micrographs by linear intercept technique. The frequency dependent initial permeability was investigated using Wayne Kerr Impedance Analyzer (Model No.6500B). The complex permeability measurements on toroid- shaped samples were carried out at room temperature in the frequency range 100Hz-120MHz. The real part (μ_i') and the imaginary part (μ_i'') of the complex permeability were calculated using the following relations $\mu_i' = L_s/L_o$,and $\mu_i'' = \mu_i' \tan\delta$, where L_s is the self inductance of the sample core and $L_o = (\mu_o N^2 h/2\pi)\ln(r_o/r_i)$, is derived geometrically. L_o is the inductance of the winding coil without the sample core, N is the number of turns of the coil (N = 4), h is the thickness, r_o is the outer radius and r_i is the inner

radius of the toroid shaped sample. DC magnetization measurements were made by using the SQUID magnetometer. B-H loops measurements were done at room temperature using an Automatic Magnetic Hysteresis Graph Tracer (AMH-300, Laboratorio Electrofisico, Italy). The B-H loops were traced from the toroid shaped samples with primary and secondary windings of ratio 40:10 and sufficient high applied field to get magnetic saturation.

4. Results and Discussion

4.1 Lattice Parameter, Density and Porosity

Fig.1 depicts the XRD patterns of various chromium-substituted Mn-Zn ferrites. The patterns exhibit typical reflections of (111), (220), (311), (222), (400), (422), (511) and (440) planes indicating the formation of cubic spinel structure. No secondary peaks were detected in XRD patterns of above mentioned samples which ensured the phase purity of each composition. The a_0 was determined by using the Nelson-Riley function, which can be expressed as $F(\theta) = 1/2\left[\cos^2\theta/\sin\theta + \cos^2\theta/\theta\right]$, where θ, the Bragg's angle. The exact values of lattice parameter of each sample was estimated from the extrapolation of all peaks to $F(\theta) = 0$ or $\theta = 90°$. It is observed that as the Cr^{3+}substitution increases, the a_0 decreases. It is due to the fact that the ionic radius of substituting Cr^{3+} (0.62Å) is less than that of Fe^{3+} (0.64Å) reported by Syue et al. (2011) and Praveena et al. (2010). Taking into consideration the preference of Cr^{3+} to the octahedral site, the partial replacement of Fe^{3+} by Cr^{3+}causes a slight effect on the unit cell dimensions was studied by Praveena et al. (2009). Similar result has been reported in Cr^{3+} doped Ni-Zn ferrite prepared by combustion synthesis by Subramani et al. (2009).

Density plays an important role in controlling the properties of polycrystalline ferrites. Fig. 2 shows the effects of Cr^{3+} on bulk density and porosity in Mn-Zn-Cr ferrites. The ρ_B decreases with increase in Cr^{3+} content, while porosity increases. The decrease in ρ_B can be attributed to the difference in atomic weight and density of the ferrite components. The atomic weight and density of Cr^{3+} (51.996 amu and 7.19 g/cm^3) respectively is less than that of Fe^{3+} (55.85 amu and 7.87 g/cm^3) reported by Subramani et al.(2009). It is found that the theoretical densities are higher in magnitude than corresponding bulk densities. This may be due to the presence of pores in the samples as investigated by Latorre-Esteves et al. (2009). The increase in P with the addition of Cr^{3+} content may be due to the creation of more cation vacancies with the reduction of oxygen vacancies as reported by Albuquerqe et al. (2002). It is observed that ρ_B of all samples increase with increasing T_s while porosity follows the opposite trend. During the sintering process, the thermal energy generates a force that drives the grain boundaries to grow over pores, thereby decreasing the pore volume and densifying the material. Highest densities of the compositions were obtained sintering at 1350 ºC.

Figure 1: The XRD Patterns of Various $Mn_{0.50}Zn_{0.50}Cr_xFe_{2-x}O_4$ Ferrites

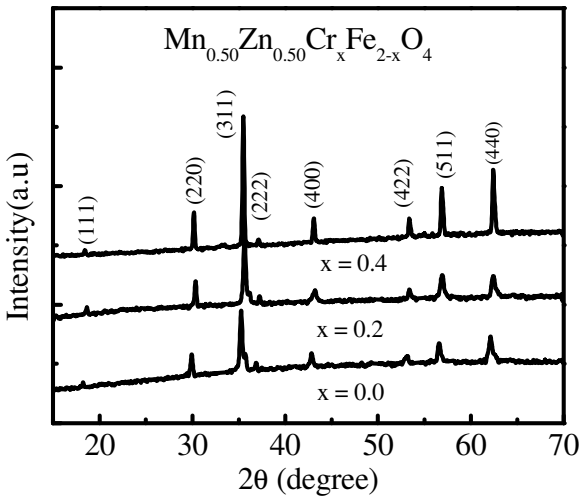

Figure 2: The Variation of Density and Porosity of $Mn_{0.50}Zn_{0.50}Cr_xFe_{2-x}O_4$ Ferrites Samples Sintered at Different Temperatures

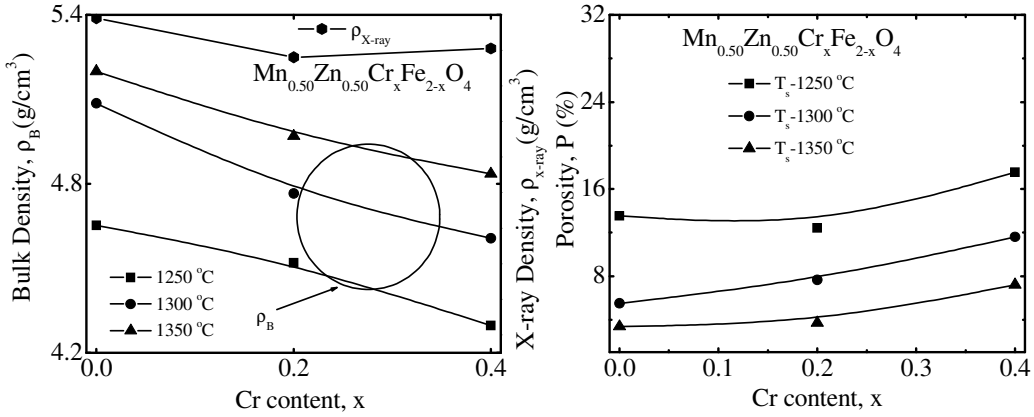

4.2 Microstructures

The surface morphology of $Mn_{0.50}Zn_{0.50}Cr_xFe_{2-x}O_4$ ferrite sample is observed by high resolution optical micrograph (Olympus DP-70) for determining the average grain size of the samples. Grain size is an important parameter affecting the magnetic properties of ferrites. The micrographs shown in Fig. 3 reveal that the grain size is influenced by the sintering temperatures. The average grain sizes vary from 3.4 to 5.7μm. The grain size increases with increase in sintering temperature can reasonably be explained on the basis of sintering mechanism. The behavior of grain growth reflects the competition between the driving force for grain boundary movement and the retarding force exerted by pores as discussed by Low and Sale (2002). When the driving force of the grain boundary in each grain is homogeneous, the sintered body attains a uniform grain size distribution. Average grain sizes of the samples are determined by linear intercept technique shown by Mendelson (1969).

Effects of sintering temperature on grain growth of $Mn_{0.50}Zn_{0.50}Cr_{0.4}Fe_{1.6}O_4$ ferrite has been investigated and is shown in Fig. 3. The average grain size increases with increasing sintering temperatures. This is because during the sintering process, the thermal energy generates a force that drives the grain boundaries to grow over pores, thereby decreasing the pore volume and increasing the grain sizes.

Figure 3: Optical Micrographs of $Mn_{0.50}Zn_{0.50}Cr_{0.4}Fe_{1.6}O_4$ Sintered at Different Sintering Temperatures

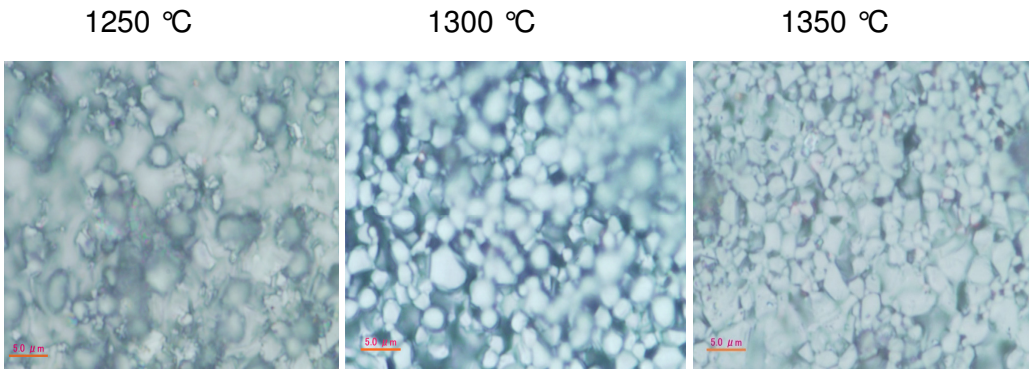

4.3 Frequency and Temperature Dependence of Complex Permeability

Fig. 4 shows the initial permeability spectra as a function of frequency for $Mn_{0.50}Zn_{0.50}Cr_xFe_{2-x}O_4$ ferrite sintered at 1250, 1300 and 1350º C. The complex permeability is given by $\mu^* = \mu_i^{/} - i\mu_i^{//}$, where $\mu_i^{/}$ and $\mu_i^{//}$ are the real and imaginary parts of complex permeability, respectively. $\mu_i^{/}$ describes the stored energy expressing the component of magnetic induction B in phase and $\mu_i^{//}$ describes the dissipation of energy expressing the component of B 90° out of phase with the alternating magnetic field H. From Fig.4, it is seen that $\mu_i^{/}$ remains almost flat until the frequency is raised to a certain level and then drops fairly to very low at higher frequencies. $\mu_i^{//}$ gradually decreases with frequency and took a broad maximum at a certain frequency, where $\mu_i^{/}$ rapidly decreases. The frequency at which $\mu_i^{/}$ attain the highest value is known as the resonance frequency. Resonance frequency is the indicator of its utility range up to which the material can be used efficiently. At the resonance, maximum energy is transferred from the applied field to the lattice resulting in the rapid increase in loss factor (tanδ) as shown in Fig. 5. It is also observed from Fig. 4 that the higher the permeability of the specimen, the lower the frequency of the resonance as observed by Snoek (1948).The values of $\mu_i^{/}$ of $Mn_{0.50}Zn_{0.50}Cr_xFe_{2-x}O_4$ sintered at 1250ºC decreases with increase in chromium ion content. Similar trend is followed in Cr^{3+} substituted Li-Sb ferrites as investigated by Laishram and Prakash (2006). It is well known that the permeability of polycrystalline ferrite is related to two magnetizing mechanism: domain wall motion and spin rotation. The domain walls normally remain pinned to the grain boundary and bulged when subjected to any small magnetic as described by Globus et al. (1971). It was assumed that the permeability due to the wall motion is likely to be linearly dependent on the grain size, while the permeability contribution due to spin rotation was assumed to be independent of grain size. Globus et al. (1971) studied several Ni-Zn ferrites and found a linear relationship between permeability and grain size (D). Perduijin and Peloschek (1968), Peloschek and Perduijin (1968) also found a linear relation

between μ_i' and D in many Mn-Zn and substituted Mn-Zn ferrites. The permeability due to domain wall motion can be expressed by Globus et al. (1971) relation $\mu_i' \propto \left(M_S^2 D / \sqrt{K_1}\right)$, where M_s is the saturation magnetization; K_1 is the anisotropy constant. Thus the domain wall motion is greatly affected by the average grain size. This is because bigger grains tend to contain large number of domain walls and μ_i' being a result of the easy reversal of domain wall displacement in the direction of the applied magnetic field. As the number of walls increases with the grain sizes, the contribution of wall movement to magnetization is increased. In our present study of microstructure, it is seen that the grain size increases significantly with increase in sintering temperature. Therefore the increase of μ_i' with increasing sintering temperature is justified. Fig. 6(a) shows the variation of permeability at different frequencies and at different T_s of of various $Mn_{0.50}Zn_{0.50}Cr_xFe_{2-x}O_4$ ferrites. There is a decreasing trend in permeability with increase in frequency. This is because at higher frequencies nonmagnetic impurities between grains and intragranular pores act as pinning points and increasingly hinders the motion of spin and domain walls thereby decreasing their contribution to permeability and also increasing the loss (Hossain and Rahman, 2011; Globus et al., 1971). It is observe from Fig. 6(b) that μ_i' increases with increase in sintering temperature T_s. This increase in μ_i' with increasing T_s is attributed to the contribution of domain wall motion, which becomes more significant as the sintered density and grain size increases. Generally, a higher μ_i' is obtained through the control of both the composition and microstructure which depends on sintering conditions. The μ_i' as a function of temperature for various $Mn_{0.50}Zn_{0.50}Cr_xFe_{2-x}O_4$ sintered at 1300 ºC is shown in Fig. 7. It is observed that there is a sudden drop in μ_i' at $T_{N,}$ where magnetic state of the ferrite changes from ferrimagnetic to paramagnetic state. This is due to the fact that at $T_{N,}$ the thermal agitation is so high that it reduces the alignment of the magnetic moment along a given axis to zero also observed by Overshott (1981).

Figure 4: The Variation Real Part and Imaginary Part of Initial Permeability of $Mn_{0.50}\,Zn_{0.50}\,Cr_x\,Fe_{2-x}\,O_4$ Sintered at 1250º C

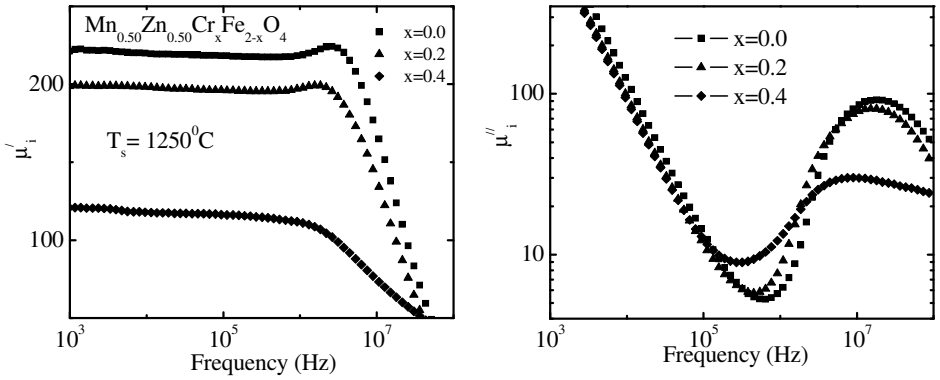

Figure 5: The Variation of Loss Factor of $Mn_{0.50}Zn_{0.50}Cr_xFe_{2-x}O_4$ Ferrites

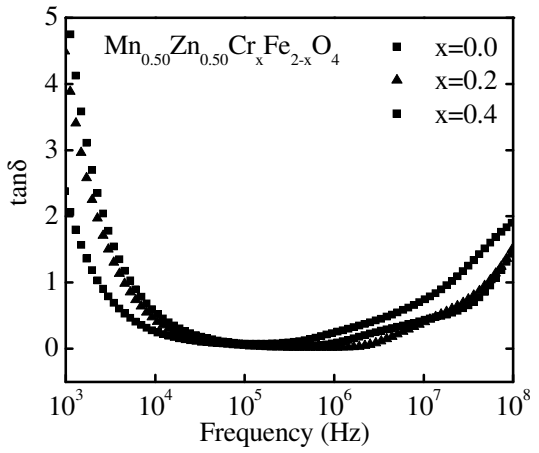

Figure 6: The Variation of $\mu_i^{/}$ of $Mn_{0.50}Zn_{0.50}Cr_xFe_{2-x}O_4$ at Different Frequencies, Samples Sintered at Different Temperatures

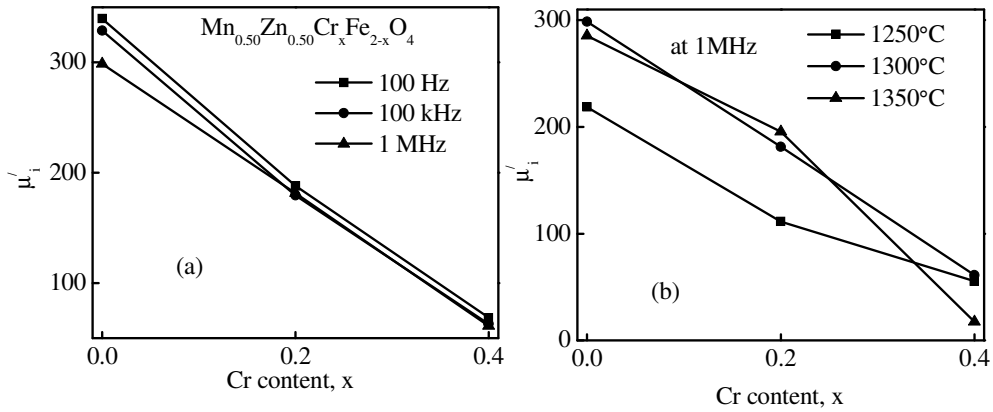

Bhosale et al. (1999) investigated that the replacement of Fe^{3+} ions by the paramagnetic or diamagnetic ions results in the fall of T_N in ferrites. The observed variations in T_N may be explained on the basis of exchange interactions. When Fe^{3+} ions at B site are being replaced by antiferromagnetic Cr^{3+} ions, B sub lattice magnetization decreases without affecting the A sub lattice magnetization, which in turn weakens A-B exchange interaction. The sharp drop of the initial permeability at T_N can be used as a measure of the degree of compositional homogeneity according to Globus et al. (1971).

Figure 7: Temperature Dependent Initial Permeability Spectra for Various $Mn_{0.50}Zn_{0.50}Cr_xFe_{2-x}O_4$ Ferrites

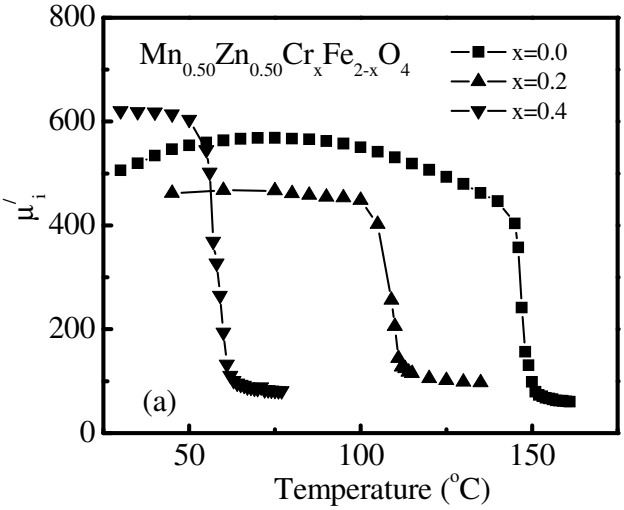

The magnetization (M) as a function of applied magnetic field (H) for various $Mn_{0.50}Zn_{0.50}Cr_xFe_{2-x}O_4$ ferrites measured at room temperature is shown in Fig. 8. The magnetization of all samples increases linearly with increasing the applied magnetic field up to 0.1T. Beyond this applied field magnetization increases slowly and then saturation occurs. It indicates that all the samples are in ferromagnetic state. The saturation magnetization, M_s, for all sample are determined by the extrapolation of magnetization curve to $\mu_\circ H = 0$.The saturation magnetization is observed to decrease with increasing Cr^{3+} content throughout the concentration range studied. It is well known that Cr^{3+} ions preferably occupy B sites as investigated by Neel [1948]. As the number of Fe^{3+} ions at B sites continuously decreases, the magnetization of B sub lattice decreases which results into the observed decrease in saturation magnetization as observed by Neel (1948). A graph has been plotted here relating to M_s and n_B with Cr content in $Mn_{0.50}Zn_{0.50}Cr_xFe_{2-x}O_4$ is shown in Fig. 9. It is seen that with increase in Cr content, both saturation magnetization and number of Bohr magnetons decrease with the substitution of Cr content. A similar decrease was reported in Mn-Zn-Cr by Rameijin (1953) and in Mg-Mn-Cr ferrites by Rao (1981).

Figure 8: Plot of the Magnetization versus the Applied Magnetic Field for $Mn_{0.50}Zn_{0.50}Cr_xFe_{2-x}O_4$ samples sintered at 1300 °C in air

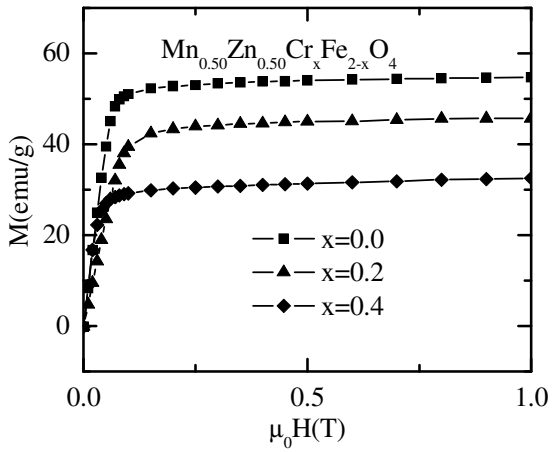

Figure 9: Variation of M_s and n_B with Cr^{3+} Content of Various $Mn_{0.50}Zn_{0.50}Cr_xFe_{2-x}O_4$ Ferrites

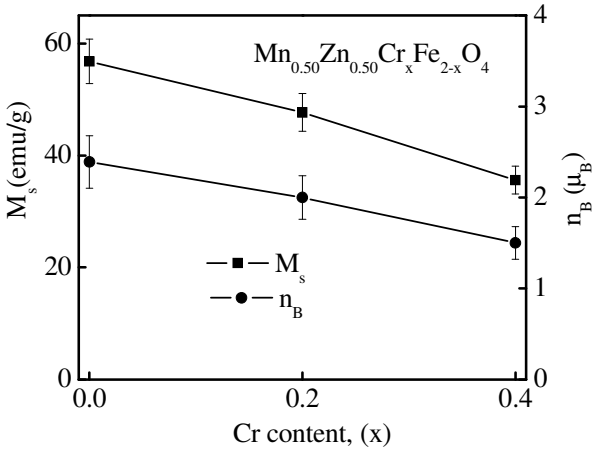

Figure 10: B-H Loops of Various $Mn_{0.50}Zn_{0.50}Cr_xFe_{2-x}O_4$ at Room Temperature, Sintered at 1350 °C. The Inset: Loops at Low Field

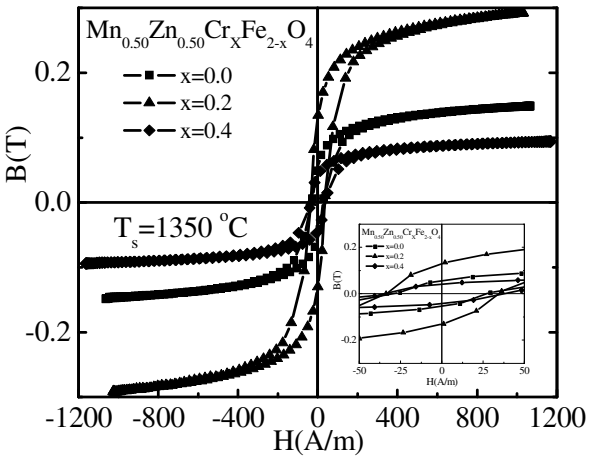

The B-H loops of Mn-Zn-Cr ferrite were recorded by a computer interfaced hysteresis loop tracer at room temperature at constant frequency. Fig.10 shows the B-H loops of $Mn_{0.50}Zn_{0.50}Cr_xFe_{2-x}O_4$ sintered at 1350 ºC. The inclusion of Cr^{3+} and various T_s significantly changes hysteresis parameter like H_c, B_r, B_s etc. H_c increases with increase in Cr but decreases with increases in T_s. The addition of Cr reduced the M_s as expected as it reduces the density of magnetic ions at B site. H_c increases due to the weakening of exchange interaction and the loss of magneto crystalline anisotropy. It is well known that all these properties are extrinsic, which depend on the grain size, intra- and inter-granular porosity. It is observed that remanence varies inversely with porosity and this agrees with the reported observations observed by Igarashi and Okazaki (1977). H_c is inversely proportional to D and μ_i' of the ferrite system as shown in Fig. 11. Our present observations of compositional variation of coercivity, initial permeability and average grain size agree with the reported value by Singh (2003).

Figure 11: Variation of H_c and $\mu_i^/$ of Various $Mn_{0.50}Zn_{0.50}Cr_xFe_{2-x}O_4$ with Cr^{3+} Content Sintered at Different Sintering Temperatures

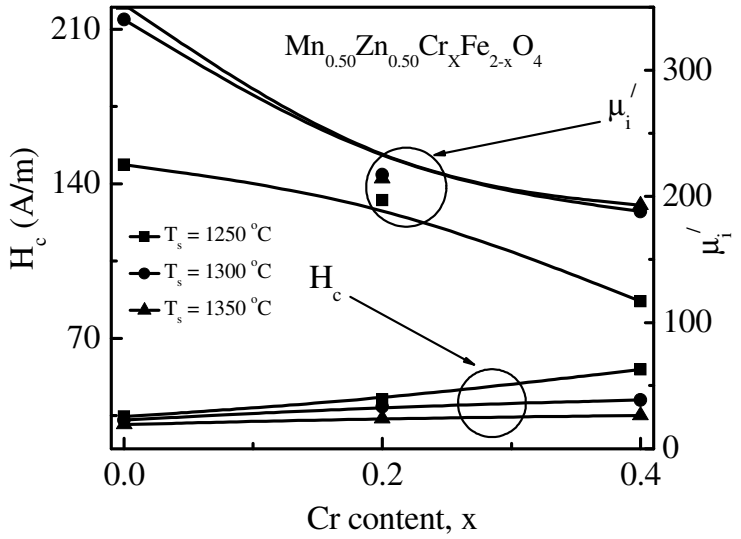

5. Conclusions

The ferrite sample prepared by auto combustion method is of single phase cubic spinel structure that has been confirmed from X-ray diffraction pattern. Substitution of Cr in Mn-Zn ferrite results in slight shrinkage of the unit cell. The grain size, ρ_B, $\mu_i^/$, T_N, decrease with Cr content but increase with increase in sintering temperatures. Initial permeability increases with increase in sintering temperature which is attributed to the increased density and average grain size of the sample. The f_r indicates the operational frequency limit of the ferrites in applications, so it is preferable to push this frequency to the higher frequency region. So the operational frequency range is increased with the increase in Cr substitution. Saturation magnetization was found to decrease with Cr content in the ferrites. Coercivity increases, retentivity and hysteresis loss decreases at the Cr rich Mn- Zn ferrite. As the hysteresis loss decreases, these low loss materials can be used in switched mode power supplies and also in radio frequency transformers and inductors. The method of fabrication of ferrite we used in this research can be used to get fine nano particles. Further studies on different characteristics are possible for fundamental interest of the studied sample. Neutron diffraction analysis may be performed for these compositions to determine the distribution of ions between A- and B- sites.

References

Albuquerque, A. S., Ardisson, J. D., Macedo, W. A. A., and Alves, M. C. M., 2002, 'Nanosized powders of NiZn ferrite: Synthesis, structure, and magnetism', *Journal of Applied Physics*, *Vol. 87, Pp. 4352-4357*.

Babbar, V. K., and Puri, R. K.,1992, 'Hot-Pressed Mn-Zn-Ni and Mn-Zn-Co ferrites for magnetic recording heads', *IEEE Transactions on Magnetics*, *Vol. 28, No.1, Pp. 21-26, 1992.*

Bhosale, D. N., Sawant, S. R., Gangal, S. A., Mahajan, R. R., and Bakare, P. P., 1999, 'Synthesis of copper–magnesium–zinc ferrites and correlation of magnetic properties with microstructure', *Materials Science and Engineering* B, *Vol. 65, Pp. 79-89.*

Cahn, R. W., Haasen, P., and Kramer, 1994, '*Materials Science and Technology*', Vol. 3B, VCH Publisher Inc., New York (USA).

Craik, D. J., 1975, *Magnetic Oxide, part 1*, John Wiley & Sons, Ltd., Bristol, England.

Dionne, G. F., and West, R., 1987, 'Magnetic and dielectric properties of the spinel ferrite system $Ni_{0.65}Zn_{0.35}Fe_{2-x}Mn_xO_4$', Journal *of Applied Physics*, *Vol. 61, Pp. 3868-3870.*

El-Sayed, H. M., 2006, 'Effect of Magnetic Field on the formation of Spin-polaron in Mn-Zn ferrites', *American Journal of Applied Sciences*, *Vol. 3, No.10, Pp. 2033-2036.*

Globus, A., Duplex, P., and Guyot, M., 1971, 'Determination of initial magnetization curve from crystallites size and effective anisotropy field', *IEEE Transactions on Magnetics*, *Vol. 7, No. 3, Pp. 617-622*.

Goldman, A., 1990, *Modern Ferrite Technology*, Van Nostrand Reinhold, New York.

Hossain, A. K. M. A., Biswas, T. S., Mahmud, S. T., Yanagida, T., Tanaka, H., and Kawai, T., 2009, 'Enhancement of initial permeability due to Mn substitution in polycrystalline $Ni_{0.50-x}Mn_xZn_{0.50}Fe_2O_4$', *Journal of Magnetism and Magnetic Materials*, *Vol. 321, Pp. 81-87*.

Hossain, A. K. M. A., and Rahman, M. L., 2011, 'Enhancement of microstructure and initial permeability due to Cu substitution in $Ni_{0.50-x}Cu_xZn_{0.50}Fe_2O_4$ ferrites', *Journal of Magnetism and Magnetic Materials*, *Vol. 323, No. 15, Pp. 1954-1962*.

Igarashi, H., Okazaki, K., 1977,'Effects of porosity and grain size on the magnetic properties of NiZn ferrite', *Journal of the American Ceramic Society*, *Vol. 60, Pp. 51-54*.

Laishram, R., and Prakash, C., 2006, 'Magnetic properties of Cr^{3+} substituted Li-Sb ferrites', *Journal of Magnetism and Magnetic Materials*, *Vol. 305, Pp. 35-39*.

Latorre-Esteves, M., Cortes, A., Torres-Lugo, M., and Rinaldi, C., 2009, 'Synthesis and characterization of carboxymethy dextran-coated Mn/Zn ferrite for biomedical applications', *Journal of Magnetism and Magnetic Materials, Vol. 321 , No. 19, Pp. 3061-3066.*

Low, K. O., & Sale, F. R., 2002, 'Electromagnetic properties of gel-derived NiCuZn ferrites', *Journal of Magnetism and Magnetic Materials*, *Vol. 246, No. 1-2, Pp. 30-35.*

Mendelson, M. I., 1969, 'Average grain size in polycrystalline ceramics', *Journal of American Ceramic Society*, *Vol. 52, No. 8, Pp. 443-446*.

Nam, J. H., Hur, W. G., and Oh, J., 1997, 'The effect of Mn substitution on the properties of NiCuZn ferrites', *Journal of Applied Physics*, *Vol. 81, Pp. 4794-4797*.

Neel, L., 1948, 'Properietés magnétiques des ferrites: ferromagnétisme et antiferromagnétisme', *Annales de Physique*, *Vol. 3, Pp. 137-198*.

Nelson, J. B., and Riley, D. P., 1945, 'An experimental investigation of extrapolation methods in derivation of accurate unit-cell dimensions of crystals', *Proceedings of the Physical Society*, *Vol. 57, No. 3, Pp. 160-177*.

Overshott, K. J., 1981, 'The causes of the anomalous loss in amorphous ribbon materials', *IEEE Transactions on Magnetics, Vol. 17, Pp. 2698-2700*.

Pannaparayil, T., Marande, R., and Komarneni, S., 1991, 'Magnetic properties of high- density Mn-Zn ferrites', *Journal of Applied Physics*, *Vol. 69, No. 8, Pp. 5349-5351.*

Peloschek, H., and Perduijn, D., 1968, 'High-permeability MnZn ferrites with flat μ-T curves', *IEEE Transactions on Magnetics*, *Vol. 4, No. 3, Pp. 453–455*.

Perduijn, D. J., and Peloschek, H. P., 1968, 'Mn-Zn ferrites with very high frequency', *Proceedings of the British Ceramic Society*, *Vol. 10, Pp. 263-273*.

Praveena, K., Sadhana, K., Bharadwaj, S., and Murthy, S. R., 2009, 'Development of nanocrystalline Mn-Zn ferrites for high frequency transformer applications', *Journal of Magnetism and Magnetic Materials*, *Vol. 321, No.16, Pp. 2433-2437.*

Praveena, K., Sadhana, K., Bharadwaj, S., and Murthy, S.R., 2010, 'Development of nanocrystalline Mn-Zn ferrites for forward type DC-DC converter for switching mode power supplies', *Materials Research Innovation*, *Vol. 14, Pp. 56-61*.

Rameijin, F. C., 1953, 'Physical and crystallographical properties of some spinels', *Philips Research Reports*, *Vol. 8, Pp. 321-342*.

Rao, K. H., 1981, 'Electrical, magnetic and Mössbauer studies in Cr, In and Al doped zinc-manganese ferrite', *Ph. D Thesis*, Andhra University, Waltair.

Shokrollahi, H., and Janghorban, K., 2007,'Influence of additives on the magnetic properties, microstructure and densification of Mn-Zn soft ferrites', *Materials Science and Engineering B*, *Vol. 141, Pp. 91-107*.

Singh, A. K., Verma, A., Thakur, O. P., Chandra, P., Goel, T. C., and Mendiratta, R. G., 2003, 'Electrical and magnetic properties of Mn-Ni-Zn ferrites processed by citrate precursor method', *Materials Letters*, *Vol. 57, Pp. 1040-1044*.

Singh, A. K., Singh, A. K., Goel, T. C., and Mendiratta, R. G., 2004, 'High performance Ni-substituted Mn-Zn ferrites processed by soft chemical technique', *Journal of Magnetism and Magnetic Materials*, *Vol. 281, Pp. 276-280*.

Snelling, E., 1988, *Soft Ferrites*, Properties and Applications, Butter-worth and Co. (Publishers) Ltd., London.

Snoek, J. L., 1948, 'Dispersion and absorption in magnetic ferrites at frequencies above one Mc/s', *Physica*, *Vol. XIV, No. 4, Pp. 207-217*.

Spaldin, N. A., 2003, '*Magnetic Materials, Fundamentals and device applications*', Cambridge University Press, UK.

Subramani, A. K., Kondo, K., Tada, M., Abe, M., Yoshimura, M., and Matsushita, N., 2009, 'High resistive ferrite films by a solution process for electromagnetic compatible (EMC) devices', *Journal of Magnetism and Magnetic Materials*, *Vol. 321 No. 24, Pp. 3979-3983*.

Syue, M., Wei, F., Chou, C., and Fu, C., 2011, 'Magnetic and electrical properties of Mn-Zn ferrites synthesized by combustion method without subsequent heat treatments', *Journal of Applied Physics*, Vol. 109, 07A324(1-3).

Van Vleck, J., 1989, *Elements of Material Science and Engineering*, 6th Ed, Addison-Wesley Co. (Publisher) Ltd., New York.

Verway, E. J. W., and Heilmann, E. L., 1947, 'Physical properties and cation arrangement of oxide with spinel structure', *Journal of Physics and Chemistry of Solids*, *Vol. 15, No. 4, Pp. 174-180*.

Yue, Z., Zhou, J., Gui, Z., and Li, L., 2003, 'Magnetic and electrical properties of low-temperature sintered Mn-doped NiCuZn ferrites', *Journal of Magnetism and Magnetic Materials*, *Vol. 264, Pp. 258- 263*.